TECHNICAL PROGRESS REPORT

A: COVER SHEET

Name of Submitting Organization: Nuonics, Inc.
Address of Submitting Organization: 1025 S. Semoran Blvd, Suite 1093, Winter Park, FL 32792
Tel/Fax: 407-379-0164 (updated address & Tel. as of April 1, 2004)

Name & Address of Sub-Contractors: (a) University of Central Florida, 4000 Central Florida Blvd., CREOL Bldg, Orlando, FL 32816-2700 and (b) AppliCote Associates, LLC, 3259 Progress Drive A, Orlando, FL 32826.

DOE Award No.: DE-FC26-03NT41923

Project Title: Ultra-High Temperature Sensors Based on Optical Property Modulation and Vibration-Tolerant Interferometry

Dated: April 1, 2004

Principal Author: Dr. Nabeel A. Riza (email: nriza@aol.com)

Period Covered by Report: Oct.1, 2003 – March 31, 2004.
Type of Report: Semi-Annual Technical Progress Report

Nuonics, Inc., Proprietary Information Pages 4-7 and 9-31.

B: ABSTRACT

The goals of the first six months of this project were to lay the foundations for both the SiC front-end optical chip fabrication as well as the free-space laser beam interferometer designs and preliminary tests. In addition, a Phase I goal was to design and experimentally build the high temperature and pressure infrastructure and test systems that will be used in the next 6 months for proposed sensor experimentation and data processing. All these goals have been achieved and are described in detail in the report. Both design process and diagrams for the mechanical elements as well as the optical systems are provided. In addition, photographs of the fabricated SiC optical chips, the high temperature & pressure test chamber instrument, the optical interferometer, the SiC sample chip holder, and signal processing data are provided. The design and experimentation results are summarized to give positive conclusions on the proposed novel high temperature optical sensor technology.

C: TABLE OF CONTENTS

D: LIST OF GRAPHICAL MATERIALS

Fig. 1a. HTHP (High temperature (up to 1200°C) and high pressure (up to 100 atm)) cell design. 1,4: Insulator; 2: Silicon Carbide; 3: Induction Heater; 5,8: Stainless Disk; 6,7: Cooler**.**

Fig. 1b. Cylindrical aluminum test cell design to examine the performance of the reflective interferometer at room temperature.

Fig. 2a. A photograph of the fabricated room temperature cell for holding the SiC optical chip for testing the reflective interferometric measurement at room temperature.

Fig. 2b. A photograph of designed and fabricated novel high temperature and high pressure cell for high temperature and high pressure measurements.

Fig. 3 Photograph of a power supply for the induction heating coil of the HTHP cell.

Fig. 4. Basic features of a silicon carbide window implemented design. TMF – Thin metal film, RB – Reference laser beam and SB – Signal (Probe) laser.

Fig. 5. Pictures of the fabricated tungsten-coated silicon carbide windows to be used as a high temperature and high pressure sensor element. These photos show the front sides of the windows with tungsten film covering one-half of each wafer.

Fig. 6. Pictures of the fabricated tungsten-coated silicon carbide windows to be used as a high temperature and high pressure sensor element. These photos show the back sides of the windows with tungsten film covering the entire backside of each wafer designed for reflective interferometry.

Fig. 7. Vacuum chamber for diffusive thin film deposition on silicon carbide for high temperature and high pressure sensor applications.

Fig. 8. Target holder to be used in the vacuum chamber (Fig. 7) for thin film deposition.

Fig. 9. Substrate holder to be used in the vacuum chamber (Fig. 7) for thin film deposition.

Fig.10 Fundamental Design of the Proposed Interferometer that engages the SiC Optical Chip with two optical beams. This is an externally referenced baseline interferometer.

Fig.11 Proposed design of the internally referenced polarization multiplexed scanning heterodyne interferometer.

Fig.12 Laboratory system implementation of Fig.11, including use of the fabricated SiC holder shown in Fig.2a.

Fig.13 Proposed design of the internally referenced wavelength multiplexed scanning heterodyne interferometer.

Fig.14: Oscilloscope Traces of Signals output from the built wavelength multiplexed heterodyne interferometer.

Fig.15 Proposed design of the internally referenced wavelength-polarization multiplexed scanning heterodyne interferometer.

Fig.16 Proposed design of the internally referenced time-wavelength-polarization multiplexed scanning heterodyne interferometer using a tunable laser.

Table 1. Various thermo-physical, mechanical and optical properties of single crystal 6H-SiC.

E: INTRODUCTION

The purpose of this project is to develop a science base to fabricate sensors for ultra high temperature fossil fuel applications. The sensors proposed are based on the principle of the Optical Path Length (OPL) variation in a medium owing to the dependence of the optical property (e.g., refractive index) of a high temperature material, such as silicon carbide (SiC), on the temperature, pressure, or species concentration. These three thermodynamic variables can be measured by a single sensor if we understand how they individually change the refractive index of the sensor material. Since these changes can be very small, a high accuracy optical signal processing scheme is proposed for working in unison with the remote SiC sensor frontend. Specifically, a vibration-tolerant interferometric technique capable of measuring the changes in OPL with sub-nanoscale accuracy and at a high speed is investigated in this project. The proposed novel sensor technique will thus enable us to measure the desired variables remotely, accurately and rapidly.

Remote interrogation of the sensor by using a laser beam will eliminate the complications associated with electrical signal-based sensors in high temperature applications. The complications in such conventional sensors include (i) melting of the solder joint between the sensor device and the bonding wire, (ii) requirement of high temperature insulation for the electrical wires connecting the device to the electrical signal processing unit, and (iii) inconvenience in mounting or embedding the device in rotating components such as the turbine blades. A high speed optical interferometer will respond to the changes in the thermodynamic variables rapidly at microsecond speeds allowing real-time control of the combustion process.

Since a passive sensor frontend is proposed, any optically transparent high temperature material, such as a single crystal silicon carbide, diamond or sapphire, can be used as the sensor material.

At least one surface of the proposed sensor needs to be coated with a thin metal film allowing reflective interrogation via the interferometer. Such a passive sensor can be produced at a very low cost in a small (sub-millimeter) size and can be readily embedded in a small hole at the surface of any structure by using the thermal expansion/contraction stress-based fitting method. The structure could be a stationary or rotating component containing the sensor at a convenient location providing remote accessibility to the probe laser beam for interferometry.

Note that the leading fiber-optic sensors such as using fiber Fabry-Perot interference or in-fiber Bragg Gratings with wavelength-based processing require costly environmental protection of the light delivery and light return fiber [1-3]. This is because the fiber intrinsically contains both the sensing zone that must react to the changing environmental conditions (e.g., temperature) and the light delivery fiber that should stay protected and essentially unaffected from changing environmental effects (e.g., changing stresses in the long lengths of the delivery fiber could cause unexpectedly high bending losses leading to loss of detection signal). It is well known that standard low loss single mode optical fibers (SMFs) are made of glass, with transition temperatures around 475 °C, leading to unwanted softening of glass at higher temperatures, such as needed in DOE applications. Thus, there exists a dilemma for the sensor design engineer using the mentioned fiber-optic sensors. In our proposed sensor, this dilemma is removed as a free-space laser beam reads sensing parameters off the SiC sensor chip, thus producing no physical contact between the harsh environment and the light delivery and processing optics. In effect, one can imagine many low cost SiC optical chips distributed in the desired sensing zone where a scanning free-space laser beam rapidly engages these sensor frontend chips to produce signals for later data processing and environmental parameter recovery. In effect, a truly non-invasive distributed optical sensor is realized.

F: EXECUTIVE SUMMARY

Accomplishments during the first six months of this project have been achieved on three fronts, namely; design, fabrication, and preliminary testing of proposed optical sensor using SiC optical chip and interface optics.

One objective was to build a custom portable test chamber for high temperature (up to 1200°C) and pressure (up to 100 atm) testing of the proposed sensor using the SiC optical chip. The chamber must be capable of holding a SiC optical chip window that can interface with a freespace laser beam coming from the optical interferometer. Such a chamber has been successfully designed and the detailed mechanical design is presented in this report. The chamber is designed to hold one inch diameter SiC chips. The portable chamber has undergone initial tests such as successful hydro-testing (i.e., pressure is supplied by water pressure) to 2000 psi without leakage. This portable chamber can act as a general test instrument for various type of chip-based optical sensing scenarios such as DOE related initiatives. As a parallel effort, we have completed designs for a vacuum chamber, target holder, and substrate holder to deposit diffusive thin films on silicon carbide using laser-assisted evaporation.

Another first phase project objective was to design and fabricate the SiC optical chip. The design chosen for the SiC optical chip that engages with the sensing zone. Such a design of the chip efficiently and robustly engages with the freespace laser beam pair coming from the optical interferometer. The SiC optical chip has been fabricated as one two inch diameter chip for preliminary tests and two one inch diameter chips for insertion into the test chamber. Mirrored films are deposited to form high temperature mirrors on the SiC substrate. The two inch chip is optically characterized with measured front and back face reflectivities, respectively, that match the expected design numbers. The SiC thicknesses are measured. A special holder is designed and fabricated for the two inch SiC chip that can be interfaced to the optics for testing.

The related first phase project objective was to design, fabricate, and conduct preliminary tests on the optical interface. The baseline interface was designed and tested using an external RF reference to measure the OPL detected by the optical chip sensor. An improved sensitivity optical interface is designed to deliver an internal referenced OPL measurement system. Both these designs are implemented in the laboratory and show a desired factor of 10 improvement in OPL detection stability. A new optical measurement architecture is proposed that has the capability to take three independent OPL measurements off the SiC chip leading to the measurement of the desired fossil fuel parameters of temperature, pressure, and species. An efficient optical architecture is proposed that generate a full data set to generate advanced sensing capabilities via the SiC chip. This aspect of the project will be required and developed during the second phase of the project.

G: EXPERIMENTAL RESULTS

G.1 Design and Fabrication of a High Temperature and High Pressure (HTHP) Cell/Chamber:

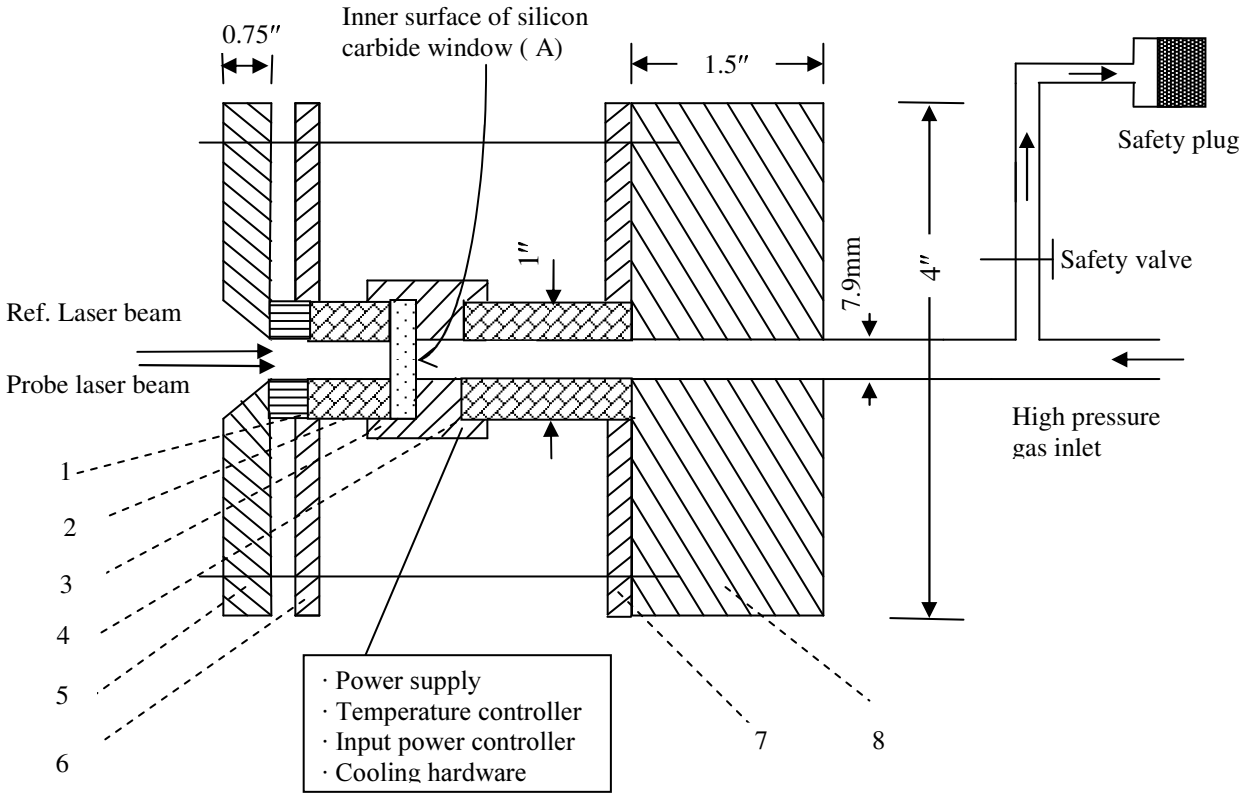

Fig. 1a. HTHP (High temperature (up to 1200°C) and high pressure (up to 100 atm)) cell design. 1,4: Insulator; 2: Silicon Carbide; 3: Induction Heater; 5,8: Stainless Disk; 6,7: Cooler.

Two important components of the sensor in this project are: (i) a high temperature (up to 1200°C) and high pressure (up to 100 atm) cell and (ii) a heterodyne vibration-tolerant interferometer interface capable of measuring the changes in the optical path length (OPL) with sub-nanoscale accuracy. A cross section of the designed HTHP cell is shown in Fig. 1a. This cell is custom designed and fabricated since such cells are commercially unavailable. The HTHP cell consists of a small (~7.9 mm diameter) hole in a stainless steel disk. The hole is covered with a heater containing a silicon carbide window. A salient feature of the novel cell is the

reduced size of the pressure cavity and small sensor exposure area, which (1) reduces the volume of hazardous chemical species and (2) reduces stress variations across the exposed sensor (window) surface.

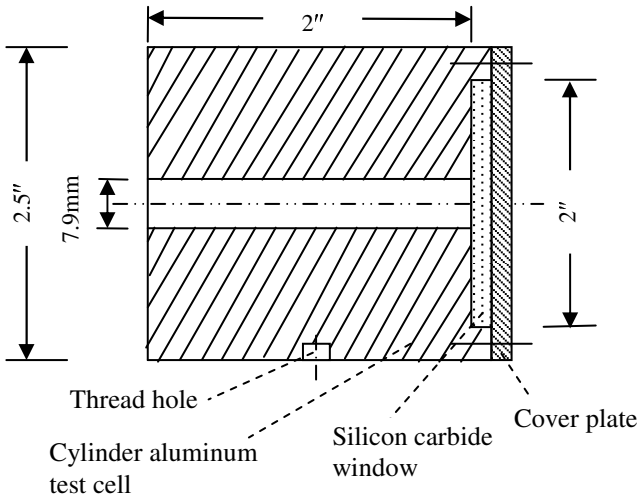

Fig. 1b. Cylindrical aluminum test cell design to examine the performance of the reflective interferometer at room temperature.

We also have designed a test cell (Fig. 1b) to evaluate the performance of the interferometer at room temperature. These cells and accessories have been fabricated as shown in Figs. 2 and 3 based on the custom cross sectional design drawings of Fig.1. Figures 2a and 2b are photographs of the room temperature cell and HTHP cell, respectively.

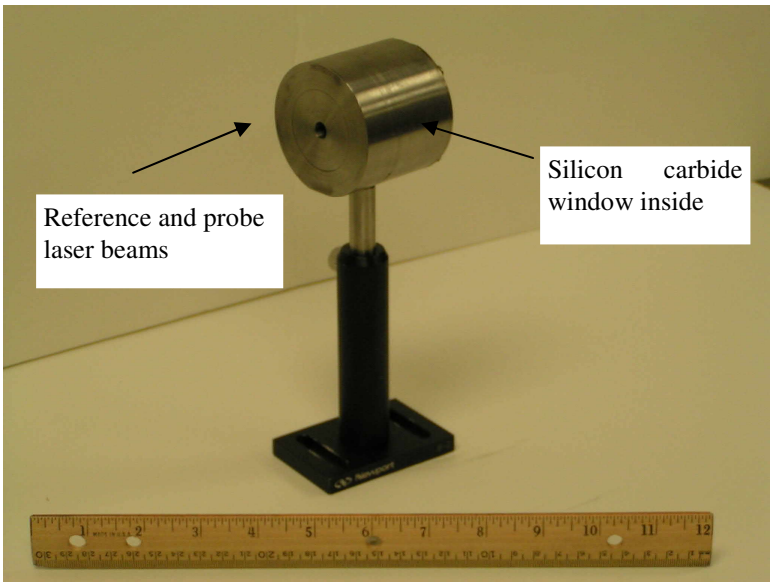

Fig. 2a. A photograph of the fabricated room temperature cell for holding the SiC optical chip for testing the reflective interferometric measurement at room temperature.

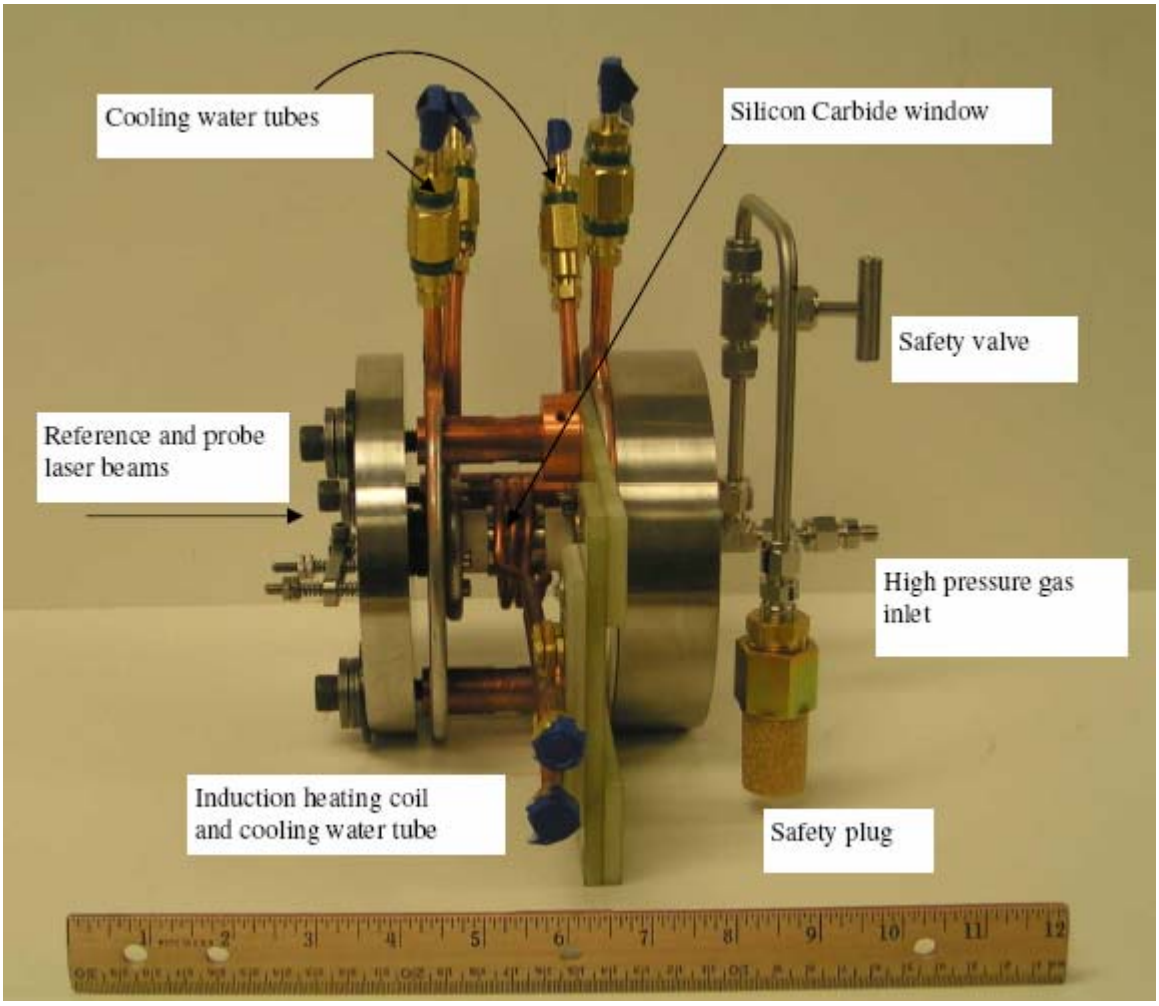

Fig. 2b. A photograph of designed and fabricated novel high temperature and high pressure cell for high temperature and high pressure measurements.

Next Fig. 3 shows the photograph of a commercial power supply to be used for the induction heating coil of the HTHP cell.

Fig. 3 Photograph of a power supply for the induction heating coil of the HTHP cell.

G.2 Design and Fabrication of a High Temperature SiC Optical Chip:

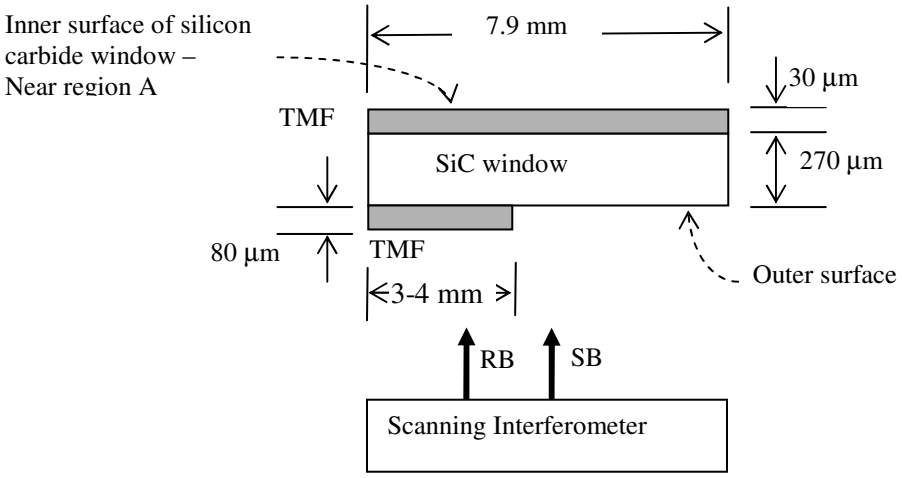

Fig. 4. Basic features of a silicon carbide window implemented design. TMF – Thin metal film, RB – Reference laser beam and SB – Signal (Probe) laser.

Figure 4 shows the implemented design of the silicon carbide (SiC) window (or optical front-end chip) with thin metal film coatings and pertinent dimensions that are later measured with a 100X optical microscope scale with a 10 micron resolution. Fig.4 also shows how basically the SiC optical chip is interrogated by the two beam of the interferometer. The inner surface (facing towards the hole, i.e., Fig. 1a & Fig.4 region A) of the window is coated with a metallic film as a circular patch to allow reflection of the probe (signal) laser beam for reflective interferometry. The outer surface of the window is coated to provide partial coverage as in Fig. 4 to allow reflection of the reference laser beam by the coating. The uncoated region of the outer surface will allow the probe beam to enter into the window and propagate towards the inner surface.

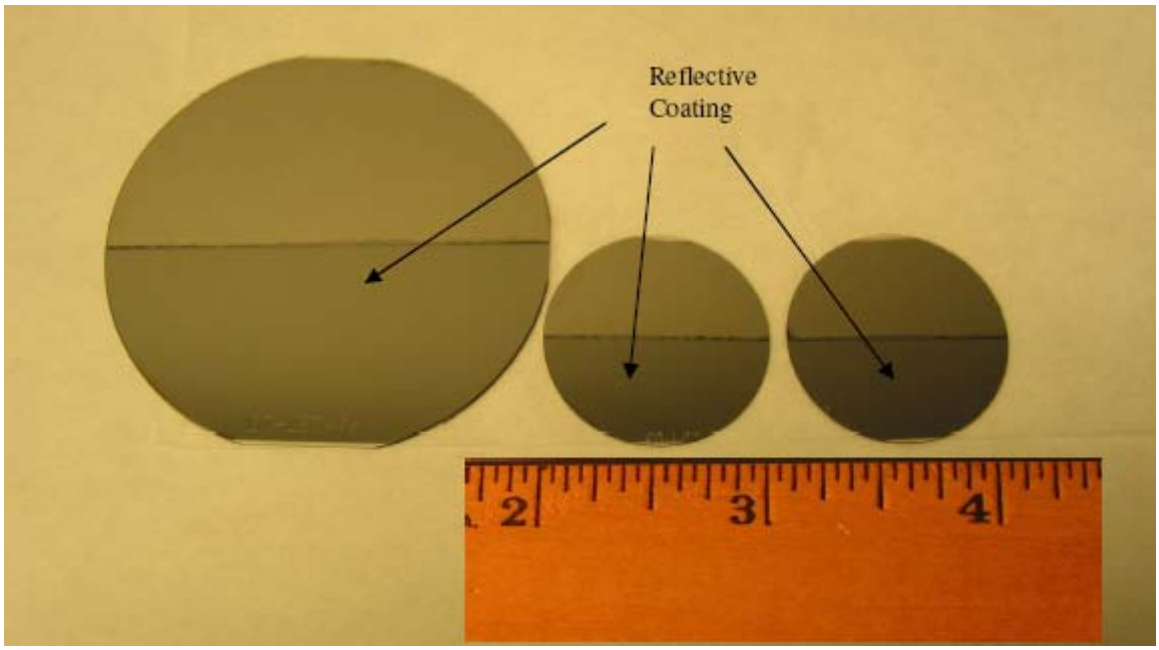

Fig. 5. Pictures of used as a high temperature the fabricated and tungsten-coated silicon carbide windows high pressure sensor element. These photos to be show the front sides of the windows with the tungsten film covering one-half of each wafer.

To expedite demonstration of been accomplished using a conventional the proposed vacuum sensor principle, preliminary metal deposition has evaporation technique. Smooth tungsten (W) metal film has been deposited to ensure a mirror finish for reflective interferometry. The complete surface of one side of the window was coated while only one-half of the opposing surface was coated. In the preliminary run, one 2-inch diameter window and two 1 inch

diameter windows were processed in this manner as shown in Fig. 5 and Fig.6. The 2-inch diameter window is for testing the interferometer at room temperature using the test cell (Figs. 1b and 2a) and the 1 inch diameter windows are for the HTHP cell (Figs. 1a and 2b) to evaluate the performance of the sensor at high temperatures and high pressures. Tungsten was chosen as the preliminary metal because of its coefficient of thermal expansion compatibility with silicon carbide (4.5 ppm/K for W versus 5.5 ppm/K for SiC over a wide temperature range of 273-1773 K) and its carbon solubility which will reduce debonding.

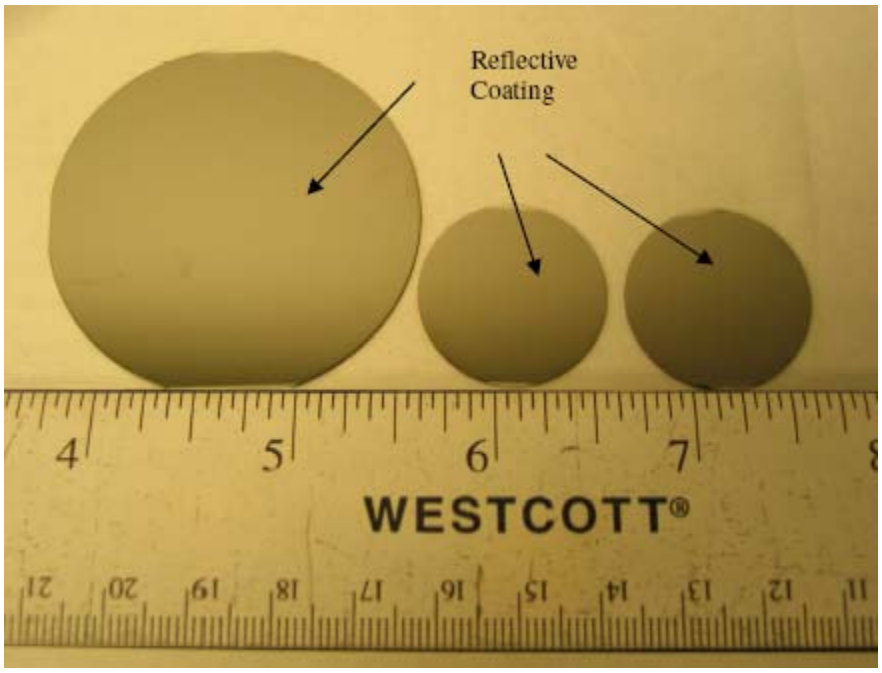

Fig. 6. Pictures of the fabricated tungsten-coated silicon carbide windows to be used as a high temperature and high pressure sensor element. These photos show the back sides of the windows with tungsten film covering the entire backside of each wafer designed for reflective interferometry.

As a parallel effort, we have completed designs for a vacuum chamber, target holder, and substrate holder to deposit diffusive thin films on silicon carbide using laser-assisted evaporation. Figure 7 shows the front and top views of the vacuum chamber with relevant dimensions. One of the windows of this chamber will be used to pass a laser beam onto one or multiple targets held by the target holder shown in Fig. 8. The other windows will be used as view-ports. The laser beam will vaporize the target material and the vapor plume will move towards the silicon carbide substrate held by the substrate holder shown in Fig. 9. The vapor will

condense on silicon carbide to form a thin film. The properties of the film and its adhesion to silicon carbide will be controlled by controlling the substrate temperature, laser irradiance at the target, target-substrate distance, and the type of inert gas and pressure inside the vacuum chamber. The vacuum chamber and associated components are currently under construction.

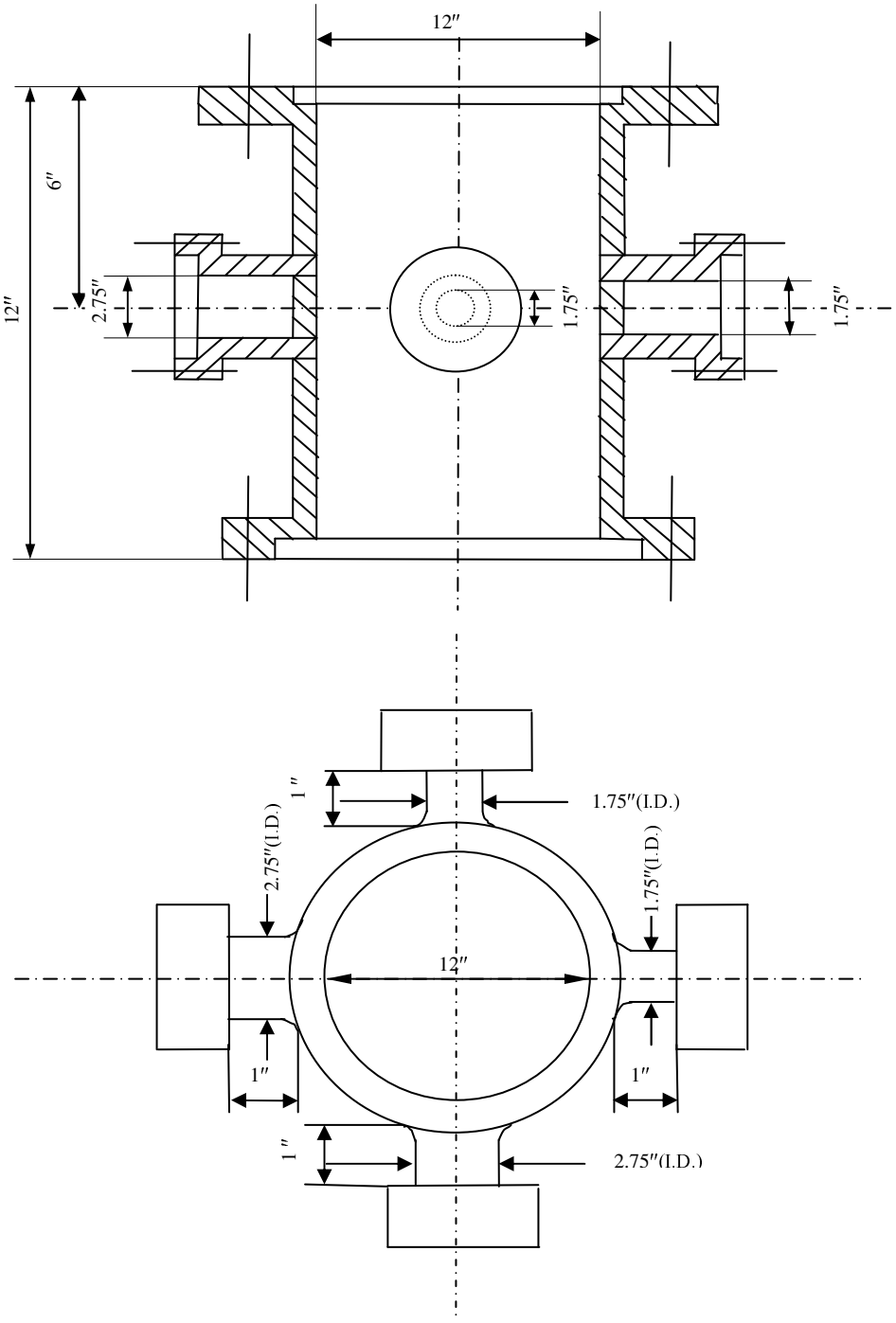

Fig. 7. Vacuum chamber design for diffusive thin film deposition on silicon carbide for high temperature and high pressure sensor applications.

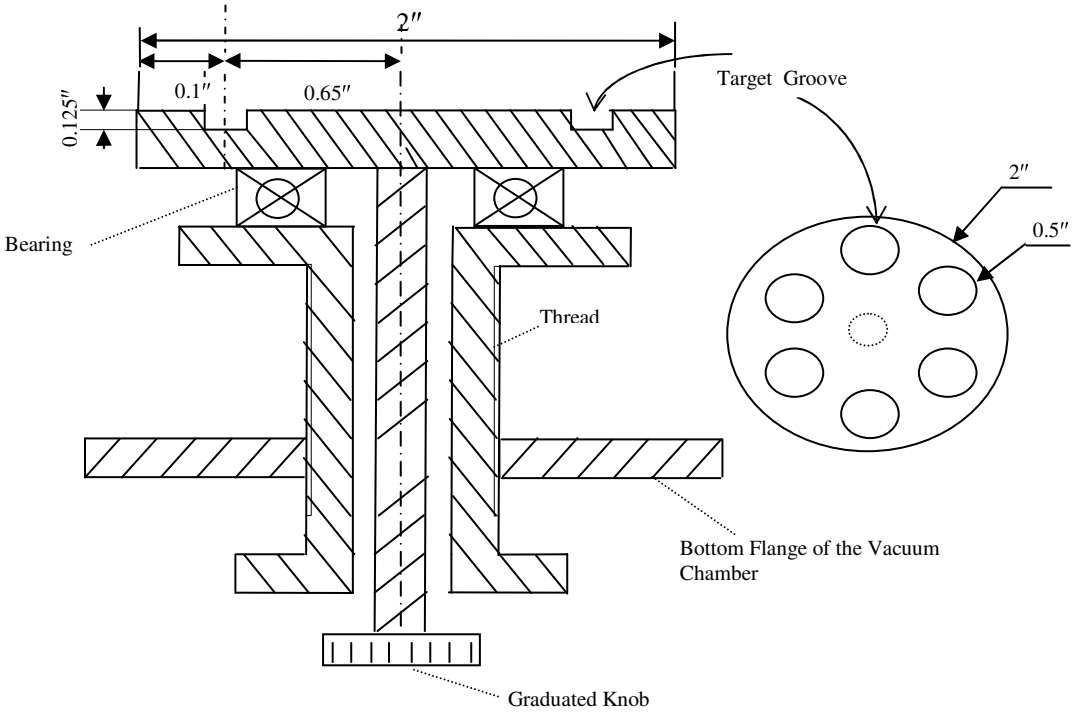

Fig. 8. Target holder design to be used in the vacuum chamber (Fig. 7) for thin film deposition.

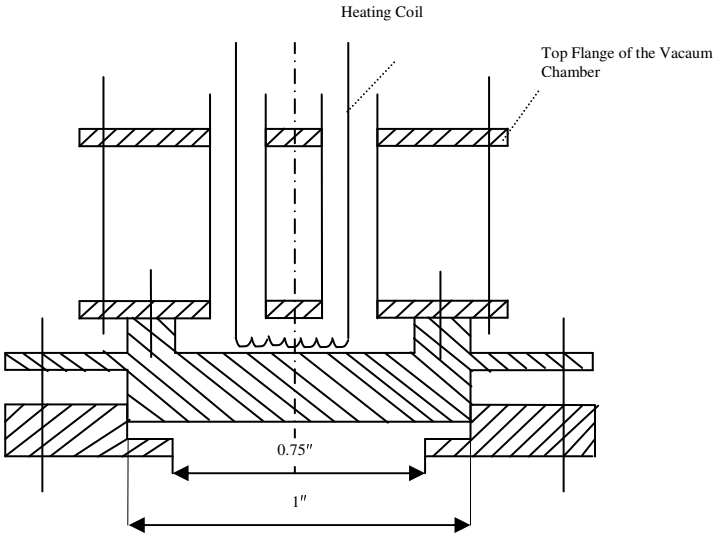

Fig. 9. Substrate holder design to be used in the vacuum chamber (Fig. 7) for thin film deposition.

G.3 Design and Fabrication of Sensor Interferometers:

The heart of the sensor measurement system is the non-invasive free-space beams based scanning heterodyne interferometer. The strength of this interferometer is its sub-nanometer scale OPL measurement sensitivity due to a vibration and environment tolerant in-line design. Furthermore, the signal laser beam can be made to electronically scan rapidly (e.g., in microseconds) in one dimension, allowing time sensitive sensor measurements or measurements at different points in space.

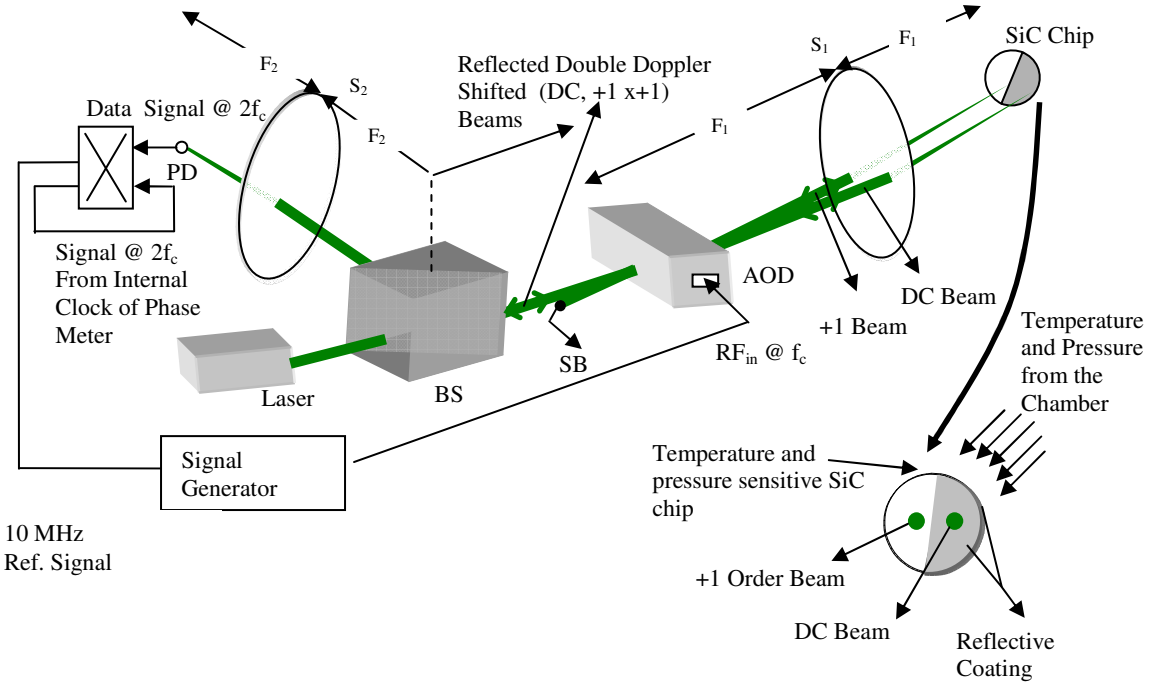

Fig.10 Fundamental Design of the Proposed Interferometer that engages the SiC Optical Chip with two optical beams. This is an externally referenced baseline interferometer.

Fig.10 shows the fundamental design of the proposed interferometer. The point to note is that only a few compact optical components quickly realizes this self-aligning self-assembly design that produces two near collinear optical beams that strike the SiC chip. The retroreflected beam pair returns via the interferometer to a single photodiode (PD) that produces the RF signal with SiC sensing parameter dependent phase shift. This phase shift is compared with an external RF signal provided via the Phase-Locking Electronics. Here, the RF of frequency f_c from a stable signal generator feeds the Bragg cell or acousto-optic device (AOD). The PD generates the phase

signal RF at $2f_c$ frequency that is fed to the lock-in electronics. The RF of frequency f_c from a stable signal generator also feeds the lock-in electronics that internally generates a stable RF at $2f_c$. Then the lock-in electronics compares the phase between the $2f_c$ frequency signals, one from the PD and one from the internal lock-in electronics.

We implemented the Fig.10 system in the laboratory as a first stage test. This system uses a flint glass AOD with a 70 MHz center frequency and 40 MHz bandwidth with a 10 microseconds aperture. The spherical lens used at the SiC optical chip plane has a 10 cm focal length. The system is first tested using a 100 mW level Ar+ ion 514 nm laser with a linearly polarized beam. A standard mirror is mounted in the SiC mount shown in Fig.2a. to gather first test data. Initial data measured from this system shows a ± 1° phase measurement stability indicating a ± 0.713 nm OPL measurement accuracy. Although this phase measurement stability achieved is good, as shown later, further improvement is possible using modified optical interferometer designs. Note that the baseline Fig.10 system uses an externally generated RF for phase referencing with the RF phase coded signal produced by the PD in the optical system. The key point is that the phase noise produced in the PD RF versus the external reference RF are not correlated. Specifically, the PD phase noise is a representation of the optical system phase noise effects including optical components and environmental conditions. On the other hand, the phase noise of the external reference RF signal is generated by the lock-in amplifier signal synthesis electronics. Because both processes are independent, their respective phase noises are uncorrelated. Hence the mixing operation in the phase meter/lock-in amplifier of the PD RF and the externally generated RF does not cancel or substantially reduce the relative phase noise in the phase difference signal that measures the OPL off the sensor optical chip.

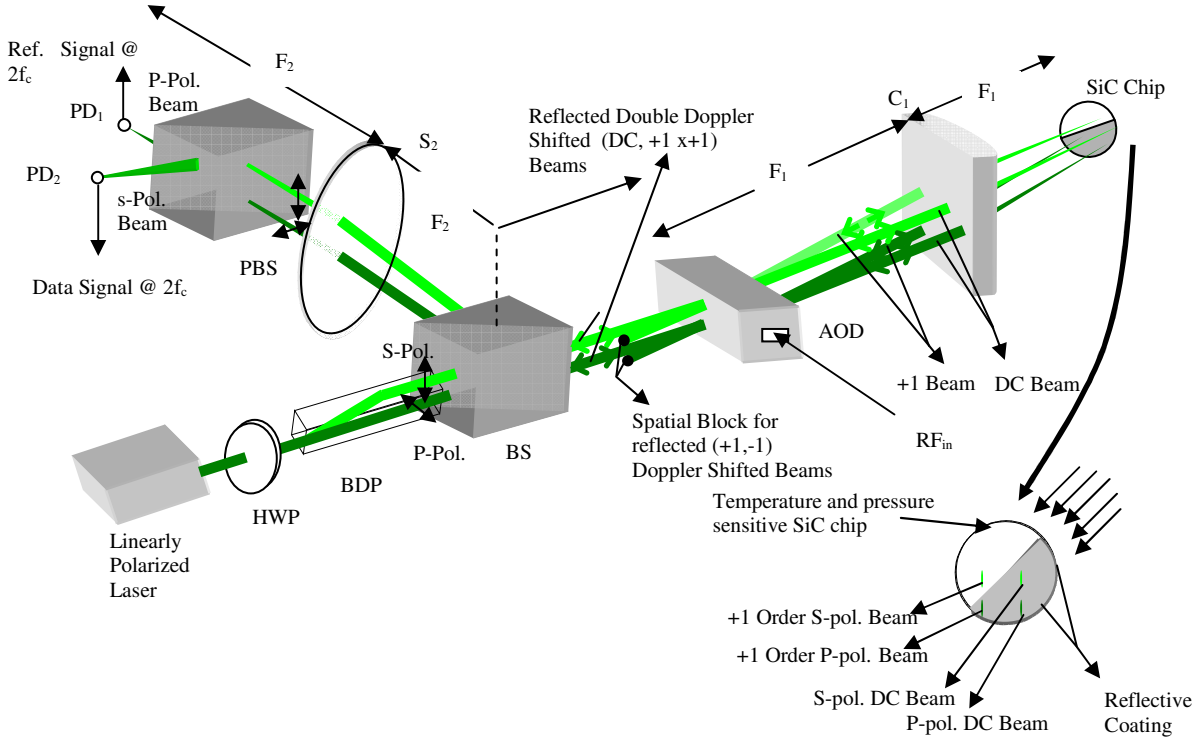

Fig.11 Proposed design of the internally referenced polarization multiplexed scanning heterodyne interferometer.

The solution to improve the OPL measurement stability rests in the ability to generate both the reference RF and signal RF from within the same optical interferometer, as shown previously in our work [4]. Because both RF signals are generated via the same optical system, their phase noises are essentially identical, leading to a higher phase stability for the eventual RF phase meter data reading. The ref.4 system used several optical components with inefficient power use to form the needed internally referenced interferometer.

Fig.11 shows a new simplified and robust design for the internally referenced interferometer. Specifically, the Fig.11 design is called the polarization multiplexed scanning heterodyne interferometer. Here, the reference RF signal and the data RF signal are created by using two orthogonal light polarizations. Specifically, a linearly polarized beam is used in conjunction with a Half Wave Plate (HWP) and a Beam Displacement Prism (BDP) at the input of the system. The HWP rotates the polarization plane of the incident beam to any desired polarization. The

function of the BDP is to create two orthogonally polarized beams (p and s polarizations) at the output face but slightly displaced from each other vertically. By varying the rotation of the HWP, the optical power of the two orthogonally polarized beams entering the AOD can be changed. This feature is highly desirable as it can be used to adjust optical powers in the two beam paths that strike the separate front and back mirror surfaces of the SiC optical chip. This power adjustment can be used to optimize PD detected RF signal-to-noise ratio. In addition, slight rotation of the BDP can be used to adjust for small misalignments with the SiC chip when the chip is taken out and then replaced for maintenance.

The Fig.11 interferometer works as follows. After passing through the BDP, the two orthogonally polarized beams that are simultaneously Bragg matched to the AOD optical and drive conditions produce two pairs of exit beams. One beam pair is p-polarized while the other is s-polarized. Each beam pair contains a diffracted/deflected beam and its corresponding DC or un-shifted beam. In effect, in the lens Fourier plane where the SiC chip is placed are present four spatially separated line beams. The height of the line beams is slightly more that the diameter of the original input laser beam; hence, these four line heights are small. The SiC chip is oriented in such a way that only the p-polarized diffracted beam passes through the SiC wafer before being retro-reflected back into the AOD. The other three beams on the SiC chip plane are retro-reflected from the front surface of the SiC optical chip. The p-polarized DC beam and the double diffracted double (+1,+1) Doppler shifted beam from the AOD combine to form a collinear beam pair that eventually generate the SiC sensing phase data signal. Similarly, the s-polarized DC beam and the double diffracted double (+1,+1) Doppler shifted beam from the AOD combine to form a collinear beam pair that eventually generate the internal reference signal for RF phase comparison. The s-polarization and p- polarization beam pairs strike a polarization beam splitter (PBS) that physically separate the signal and reference beam sets in the interferometer. After this separation, each beam pair is incident on its respective high speed photo-detector (PD) to produce its heterodyne detected RF signal at $2f_c$ where f_c is the AOD drive frequency. Hence, PD_1 generates the phase meter reference signal at $2f_c$ while PD_2 generates the phase coded sensing data signal @ $2f_c$ that is also fed to the phase meter. The relative phase between the two RF signals is measured by the phase meter/lock-in amplifier. The relative phase shift measured between these two RF signals is due to the extra optical path length traveled by the +1 order p-polarized beam that passes through the SiC substrate of the SiC optical chip. Note that because

the two beam pairs engage the same optical components, both beams suffer near identical phase noise conditions. Here the phase meter is fed by RF signals with correlated phase noise, leading to an expected improvement in phase measurement stability versus an external RF signal interferometer set-up.

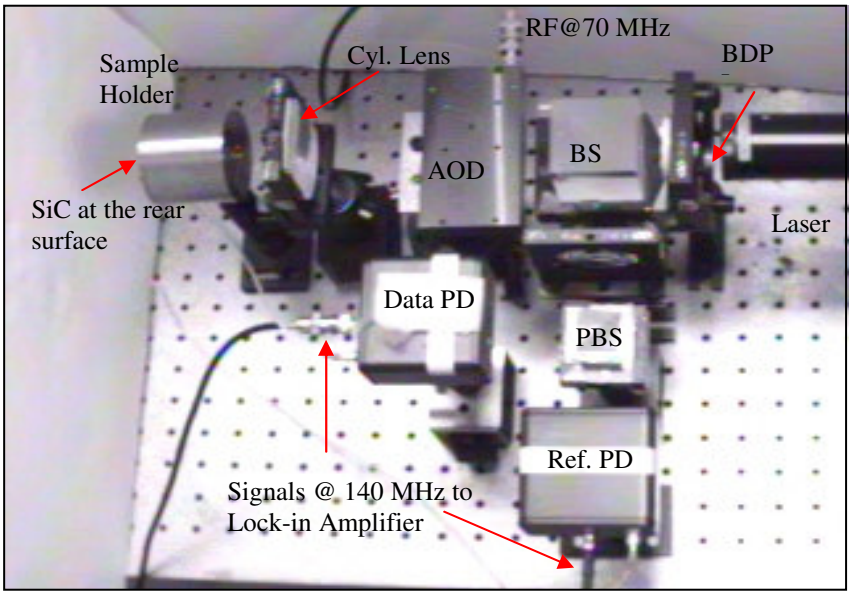

Fig.12 Laboratory system implementation of Fig.11, including use of the fabricated SiC holder shown in Fig.2a.

Next, the Fig.11 internally referenced polarization multiplexed scanning heterodyne interferometer is set-up in the laboratory, as shown in Fig.12. The AOD is fed by a 70 MHz RF and the PDs produce 140 MHz RFs that are fed to a phase meter. The cylinder used has a 10 cm focal length while the wavelength is 514 nm. The phase meter reading gives a phase measurement stability of ± 0.1° indicating a ± 0.713 Angstrom OPL measurement accuracy. Compared to the externally referenced design of Fig.10, the new Fig.11 design indeed gives a much better phase measurement stability; in fact, at present a factor of ten improvement in measurement sensitivity, thus progressing to the needed Angstrom scale OPL sensitivity. An important point to note is that the Fig.12 experiment is conducted under normal laboratory conditions with no-air flotation on the optical table, showing the robustness of the proposed interferometer design.

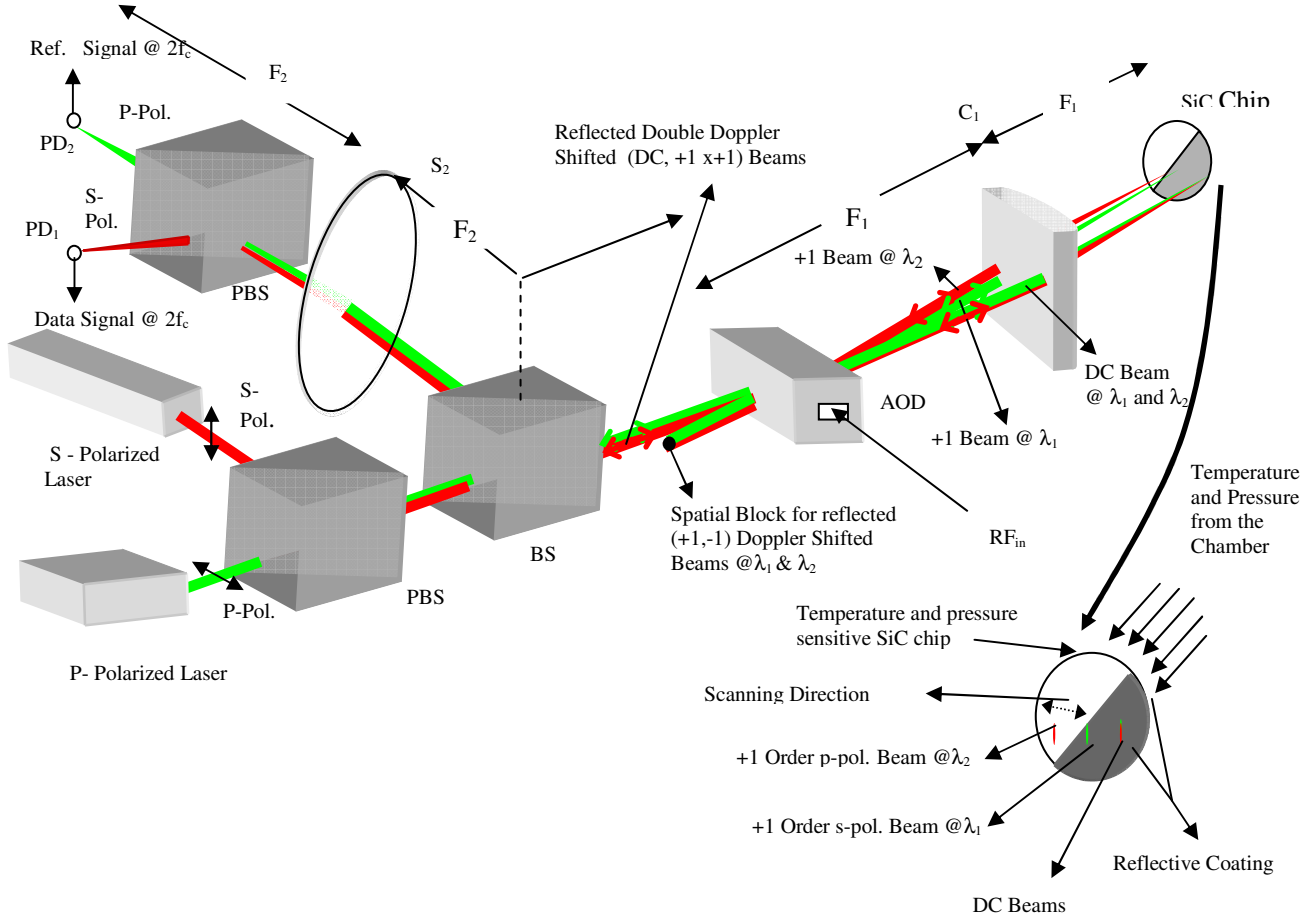

Fig.13 Proposed design of the internally referenced wavelength multiplexed scanning heterodyne interferometer.

An alternate interferometer design that keeps the two beam pairs closer to each other to reduce phase noise is shown in Fig.13. This new design uses two independent lasers at different wavelengths but orthogonal linear polarizations. Using a PBS, the starting input two laser beams are made perfectly collinear (unlike Fig.11) before entering the baseline interferometer system. Thus by making the beams exactly one on top of the other before entry into the beam splitter (BS), exactly the same phase noise is picked up, making a highly robust system in case small scale (within a millimeter scale) spatial phase perturbations are expected across beam paths. Note that in Fig.13, the two different wavelength (and polarization) beams are shown to be slightly offset from each other so they can be visualized. In reality, they are exactly one on top of each other. Here, the +1 order s-polarized red beam gets diffracted at a slightly higher angle and

thus is reflected from the back surface of the SiC optical chip. This beam then acts as the phase coded signal beam. As in the previous design, after passing through the AOD twice, a PBS is used at the output to separate the signal and reference beam pairs. PD_1 generates the reference signal at $2f_c$ from the p-polarized green beam while PD_2 generates the data signal @ $2f_c$ from the s-polarized red beam. The remaining operation of the system is as before.

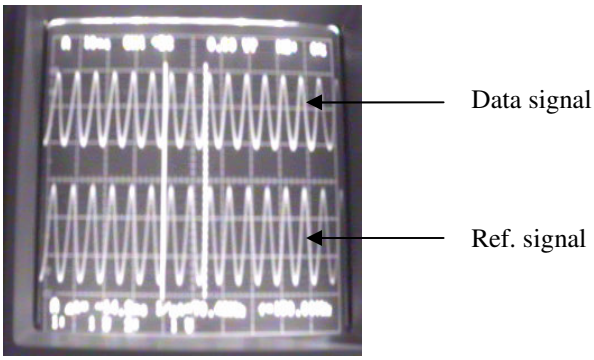

Fig.14: Oscilloscope Traces of Signals output from the built wavelength multiplexed heterodyne interferometer.

The proposed Fig.13 design of the internally referenced wavelength multiplexed scanning heterodyne interferometer is assembled in the lab. for initial testing. The wavelengths used were 633 nm red and 514 nm green. The AOD was Bragg matched for a 75 Mhz drive frequency giving two output signals at 150 MHz frequencies. Fig.14 shows the two clean RFs generated from the experimental wavelength multiplexed heterodyne interferometer. The red beam is responsible for engaging the sensing zone. As before, a flat mirror is used in the sensing zone to perform phase measurement stability experiments. The results again indicate a measurement stability of ± 0.1°. Because the red wavelength engages the sensing zone, the ± 0.1° phase stability corresponds to a ± 0.88 Angstrom OPL measurement accuracy. Again, the needed Angstrom level measurement sensitivity is achieved.

Recall that the final DOE goal is to enable measurement of temperature, pressure, and species in a high temperature fossil fuel environment. In order to enable these three measurements with the proposed SiC optical chip, one must some how taken three independent measurements of OPL via the SiC optical chip. The proposed approach for this project is to use three independent laser wavelengths to take the three OPL measurements from the same sensing zone on the SiC optical

chip. Hence proposed is a new interferometer design called wavelength-polarization multiplexed scanning heterodyne interferometer shown in Fig.15.

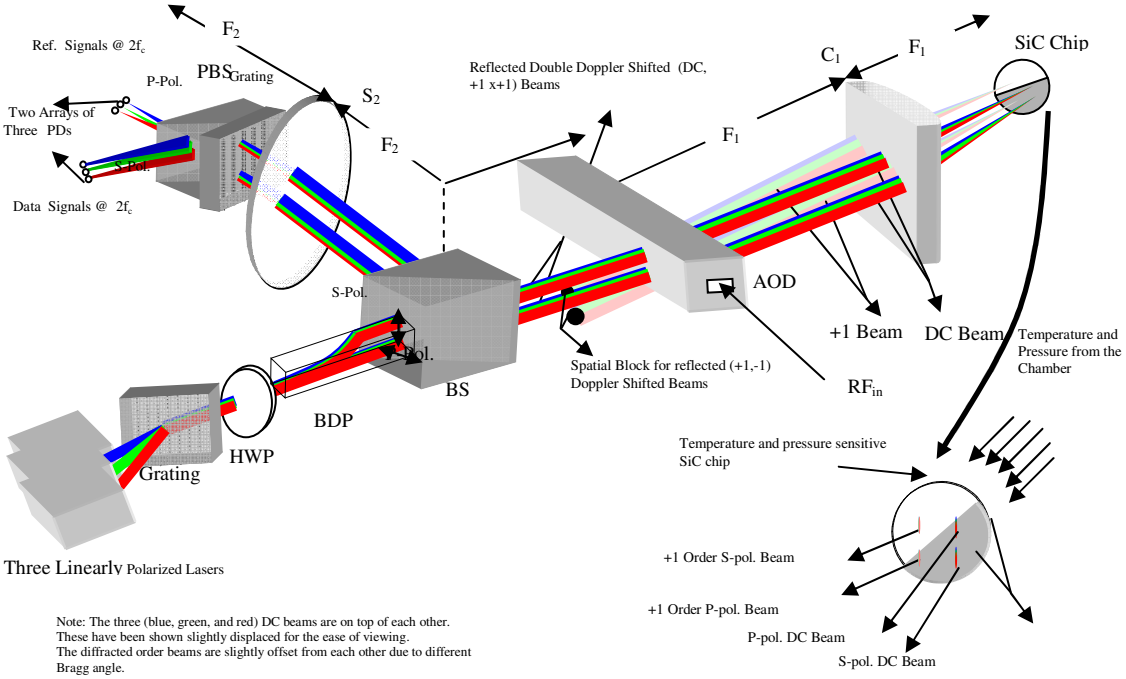

Fig.15 Proposed design of the internally referenced wavelength-polarization multiplexed scanning heterodyne interferometer.

The design in Fig.15 is a combination of the polarization multiplexed scanning heterodyne interferometer and the wavelength multiplexed scanning heterodyne interferometer. This hybrid design uses three linearly polarized lasers with three different wavelengths. Again, the rotation of a common HWP is used to control the intensity ratio between the p and s polarization components for each independent wavelength. If different ratios are required per wavelength to give full sensing flexibility, then each laser beam is accompanied by its own HWP placed before the grating. In this case, the input grating polarization dependent loss (PDL) effects must be taken into account. The three wavelengths are incident at their respective Bragg angles on the input grating, producing an output diffracted beam where the three colors are collinear and hence on top of each other. Again for clarity, in Fig.15 the three colored beams are shown slightly offset from each other. The AOD drive RF is chosen that sufficient Bragg diffraction is

achieved simultaneously for all three wavelength. At the sensor plane, the AO diffraction process produces six +1 order diffracted beams and six DC or undiffracted/deflected beams. In effect, there are six beam pairs where one beam pair contains one +1 order diffracted beam and its corresponding DC beam for the given wavelength and specific linear polarization. Of the six beam pairs, 3 beam pairs (one per wavelength) acting as the phase signal sensing signal generators are at the p-polarization while the corresponding 3 beam pairs (one per wavelength) are the internal reference signal generators and are at the s-polarization. At the output of the interferometer, after double passage through the AOD, a PBS and an output grating are used to successfully generate the required phase and reference RF signals for the three wavelengths. Thus, the proposed wavelength-polarization multiplexed scanning heterodyne interferometer indeed provides three independent OPL measurements from the sensing zone of the proposed SiC optical chip. Then these three data sets can be used to calculate the three unknown quantities of temperature, pressure, and species concentration. Note that depending on various system parameters such as wavelength values, Fourier transform cylindrical lens focal length, AOD device parameters, the diffracted beams from the three wavelengths are spatially slightly displaced. Because this displacement is expected to be small (< 100 micron), the data generated is still considered sensed over a small zone on the SiC optical chip.

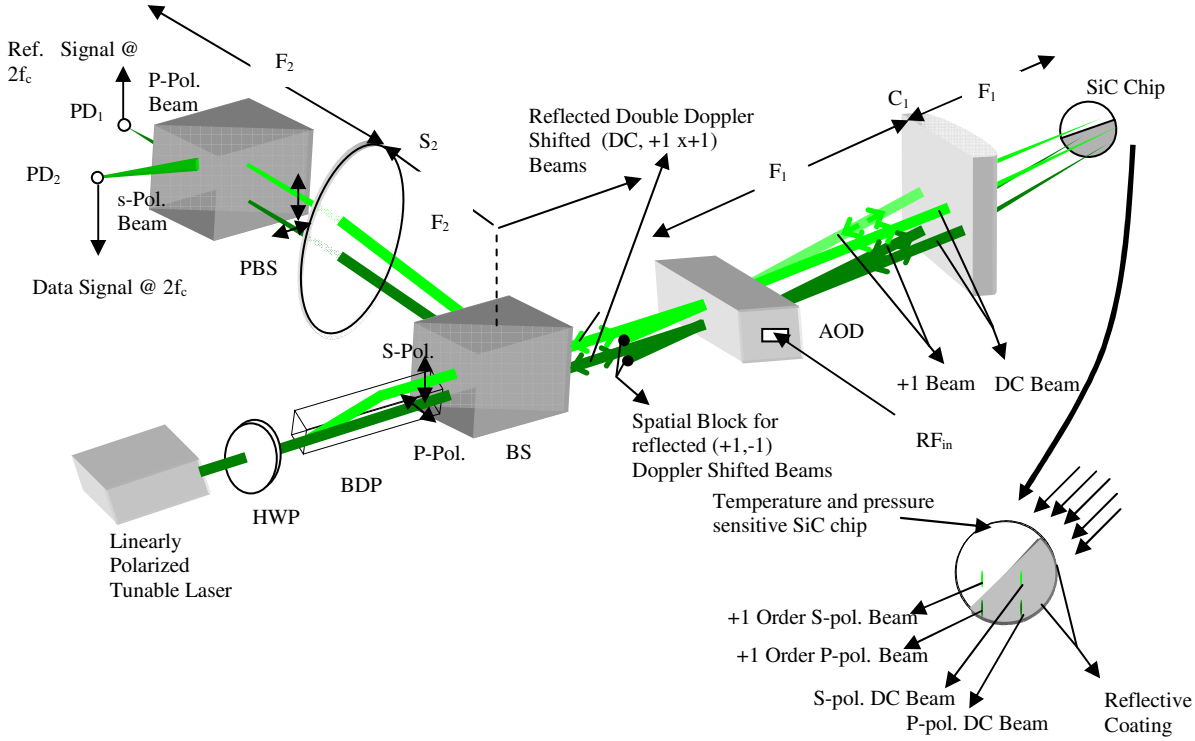

Fig.16 Proposed design of the internally referenced time-wavelength-polarization multiplexed scanning heterodyne interferometer using a tunable laser.

As shown in Fig.16, one possible modification to the Fig.15 system is the replacement of the three fixed wavelength lasers and their grating optics by a single tunable laser that in time generates multiple different wavelengths, one at a time, for time multiplexed data measurements. In this case, the optics at the input and output ports is simpler. In addition, the AOD RF drive can be changed to track the changing wavelengths, leading to possible wide band measurements over a given optical band. This modified interferometer can be called an internally referenced time-wavelength-polarization multiplexed scanning heterodyne interferometer. Because laser tuning can be obtained at high speeds, high speed time multiplexed data processing can lead to high resolution sensing by the SiC optical chip sensor. Hence, this type of interferometer is the most advanced and powerful optical interface proposed for the SiC optical chip sensor.

H: RESULTS AND DISCUSSION

This project requires a special portable high temperature and pressure chamber that can hold the designed and fabricated SiC optical chip and allow the chip to be optically interrogated by a free-space laser beam. Our team has successfully delivered this goal. Specifically, the HTHP cell has been successfully hydro-tested (i.e., pressure is supplied by water pressure) to 2000 psi without leakage. A metal blank was used to seal the window orifice. An induction heating coil (see Fig. 2a) has been fabricated for positioning over the window flange and all controls of the heating coil have been integrated into a control box.

Table 1. Various thermo-physical, mechanical and optical properties of single crystal 6H-SiC.

Properties	Values
Density (kg/m^3)	3214
Specific heat capacity (J/kg·K)	690
Thermal conductivity (W/m·K)	490
Melting (peritectic reaction) temperature (ºC)	2545 at 1 atm and 2830 at 35 atm
Linear thermal expansion coefficient ($ºC^{-1}$)	4.5×10^{-6}
Elastic modulus (GPa)*	475 at 20ºC and 441 at 1500ºC
Shear modulus (GPa)*	192
Bulk modulus (GPa)	220
Poisson ratio*	0.142
Refractive index for different wavelengths (λ) at room temperature	2.7260 for λ = 473 nm (Blue light) 2.6932 for λ = 532 nm (Green light) 2.6567 for λ = 633 nm (Red light)

*Data for 4H-SiC.

There are numerous polytypes of silicon carbide such as 3C (cubic), 2H (hexagonal), 4H (hexagonal), 6H (hexagonal) and 15R (rhombohedral). Since 6H-SiC is used as the sensor element, its relevant properties such as room temperature refractive index are listed in Table 1.

We have successfully fabricated three SiC optical chips. Approximate dimensions of the 2-inch diameter SiC fabricated window are measured as: 270 μm thick 6H-SiC wafer, 30 μm thick W film covering the entire surface of the wafer, and 80 μm thick W film covering only one-half of the wafer.

The SiC chip has also been experimentally tested for optical parameters such as reflectivity and polarization independence. Present measurements of reflectivity conducted at the red 633 nm wavelength have given a 40 % reflectivity for the front mirrored face of the chip and 30% reflectivity for the back mirrored face of the chip that also includes double passage through the front air-SiC interface. These numbers indeed match the design numbers as indicated as follows. The reflectivity number for the front face Tungsten mirror is consistent with the 30-40 % reflectivity number reported for Tungsten mirrors at 633 nm as earlier reported in the literature [5]. The air-SiC interface produces a Fresnel Transmissivity coefficient T= 1-R, where R= r^2, where for near normal incidence, r = [n (SiC)- n (air)]/ [n (SiC) + n (air)]. Here r is the Fresnel reflection coefficient, R is the Fresnel Reflectivity coefficient, n (SiC) is the refractive index for SiC at the measurement temperature and wavelength, and n (air) is the refractive index of air. Using the n(SiC)=2.6567 from Table 1 and n(air)=1, r= 0.4531 or R=0.205. This implies that T= 0.795 or that 79.5 % of light passes through an air-SiC interface. Considering the path that the light beam has to travel to strike the mirrored back side of the SiC chip, the expected transmission efficiency for this beam is 0.795 (air-SiC) x 0.4 (Tungsten) x 0.795 (SiC-Air)= 0.26 or 26 %. Here we have assumed that the back face Tungsten mirror also has the same reflectivity as the front face mirror, or 40 %. The measured transmission for this back mirror reflected beam comes to be 30 %, slightly higher than the design value of 26 %. This is because the fabricated back surface mirror and has a slightly higher fabricated reflectivity than the 40 % measured reflectivity for the front surface mirror. These initial results indicate that the SiC optical chips indeed have sufficient optical reflectivities to feed the interrogating free-space beam interferometer. In addition, any unbalanced power levels for the two retro-reflecting SiC chip beams can be balanced using optical and electronic power balancing techniques in the proposed interferometers.

For interferometric interrogation of the sensor as shown earlier in Fig.4, two laser beams are to be directed to the designed silicon carbide window. These two beams are reflected from two surfaces of the window to determine the changes in the optical path length caused by the variation in the refractive index of silicon carbide due to high pressure in region A or due to high temperature of silicon carbide. To study the effect of pressure on the refractive index of silicon carbide, region A will be filled with a high pressure gas (e.g., Argon) from a high pressure gas cylinder. The pressure of the gas in region A will be varied and the corresponding changes in the optical path length (OPL) will be determined. These data will be used to calculate the refractive index of silicon carbide as a function of gas pressure. Similarly, the silicon carbide window will be heated to different temperatures at a given gas pressure, and the corresponding changes in the optical path length will be determined to obtain the refractive index as a function of temperature.

Successful design of the optical interface to the SiC chip has been achieved. First, the baseline externally referenced interferometer is designed, built, and tested. It is shown that this type of interferometer has a nanometer-type OPL measurement stability. Next, internally referenced optical interferometer designs using polarization or wavelength multiplexing are proposed, designed, and tested, indicating a factor of ten improvement in OPL measurement stability, i.e., the Angstrom level. As the eventual project goal is measurement of three independent sensing parameters of temperature, pressure, and species using the same SiC optical chip, novel optical interfaces based on using multiple wavelengths are introduced. The first system uses three wavelengths and forms an internally referenced wavelength-polarization multiplexed scanning heterodyne interferometer. The second more advanced system forms an internally referenced time-wavelength-polarization multiplexed scanning heterodyne interferometer using a tunable laser. It is expected that these optical interfaces will engage the proposed SiC optical chip to enable advanced sensing of fossil fuel high temperature scenarios leading to project objectives over the three years. Initially in the 2nd phase of the project first year, the baseline line internally referenced optical interfaces will be used to provide temperature and pressure signals via the designed and fabricated SiC optical chips.

I: CONCLUSION

The success of the proposed project depended on several key factors during the first year phase of the project.

First, we required a way to test our proposed SiC chip sensor with high temperature and pressure conditions, all implemented within a low cost, portable test chamber. We have succeeded in achieving this goal by designing, building, and preliminary testing such a custom test chamber. The details of this test chamber have been presented in this report. As a parallel effort, we have completed designs for a vacuum chamber, target holder, and substrate holder to deposit diffusive thin films on silicon carbide using laser-assisted evaporation.

Second, for the first time to our knowledge, we have shown how an optical chip needed for high temperature and pressure sensing proposed in this project can be designed and fabricated using a SiC substrate and Tungsten mirrors. The chip design is unique as the front face of the chip is a half-mirror while the back face is a full mirror. This unique chip design allows efficient and stable interface to the free-space laser beam optics interrogating the SiC chip. The details of fabrication of the SiC optical chips have been presented in this report.

Finally, the optical interface to the SiC chip requires super resolution phase stability to detect OPL changes on an Angstrom scale. This need has been delivered in this project by designing new polarization and wavelength multiplexed optical heterodyne interferometers that provide an internal RF referencing scheme. These architectures have been built and tested, indicating the required Angstrom scale OPL measurement stability. The details of the design and fabrication of these optical interfaces have been presented in this report. In addition, ground work has been laid towards the advanced optical interface architecture that will be used to make the multiple sensing measurements (e.g., pressure, temperature, and species) via the single SiC chip. Details of this novel optical interface design are also presented in the report.

The design chosen for the SiC optical chip includes a chip frontend with half a mirror and a fully mirrored back face that engages with the sensing zone. Tungsten films are deposited to form high temperature mirrors on the SiC substrate. The two inch chip is optically characterized with

measured 40% and 30 % front and back face reflectivities, respectively, that match the expected design numbers. The SiC thicknesses measured are: Front mirror film thickness: 80 micron; Back mirror film thickness 30 micron; SiC substrate thickness: 270 micron.

Data collected from this system indicates at best a ± 1° phase measurement stability indicating a ± 0.713 nm OPL measurement accuracy using 514 nm laser. An improved sensitivity optical interface is designed that using either polarization multiplexing or wavelength multiplexing to deliver an internal referenced OPL measurement system. Specifically, data indicates a ± 0.1° phase measurement stability indicating a ± 0.713 Ansgtrom OPL measurement accuracy using 514 nm laser. A new optical measurement architecture using three wavelengths combined with polarization multiplexing is proposed that has the capability to take three independent OPL measurements off the SiC chip leading to the measurement of the desired fossil fuel parameters of temperature, pressure, and species. An efficient optical architecture that uses a wavelength tunable laser to implement a time-wavelength-polarization multiplexed optical interferometer is proposed that generate a full data set to generate advanced sensing capabilities via the SiC chip.

Next, the SiC chip will be placed in the test chamber and interfaced with the proposed internally referenced interferometer to take OPL data readings as temperature is changed and then as pressure is changed, indicating that indeed the SiC optical chip forms a robust high temperature and pressure sensor.

J: REFERENCES

[1] R. Duncan, D. Gifford, V. Rajendran, " OFDR tracks temperatures on power generators," Laser Focus World Magazine, p.89, Oct. 2003.

[2] A. D. Kersey, et.al., " Fiber Grating Sensors," IEEE/OSA J. Lightwave Tech., Vol.15, No.8, pp.1442-1463, August 1997.

[3] Brian Culshaw, " Optical Fiber Sensor Technologies: Opportunities and Perhaps Pitfalls," IEEE/OSA Journal of Lightwave Technology, Vol. 22 , No. 1, pp 39 – 50, Jan. 2004.

[4] N. A. Riza and Muzamil A. Arain, " Angstrom-range optical path-length measurement with a high-speed scanning heterodyne optical interferometer," Applied Optics, OT, Vo.42, No.13, pp.2341-2345, 1 May 2003.

[5] Yumu Sato, Seishi Sekine, and Masashi Ohkawa , "Measurement of Complex Refractive Index of Tungsten by Using Ellipsometry", IEEJ Transactions on Fundamentals and Materials, Vol. 124-A, No. 2, pp 114, Feb. 2004.